symmetry

MDPI

Article

The Geometrical Basis of $\mathcal{PT}$ Symmetry

Luis L. Sánchez-Soto [1,2,*] and Juan J. Monzón [1]

[1] Departamento de Óptica, Facultad de Física, Universidad Complutense, 28040 Madrid, Spain; jjmonzon@opt.ucm.es

[2] Max-Planck-Institut für die Physik des Lichts, Staudtstraße 2, 91058 Erlangen, Germany

* Correspondence: lsanchez@fis.ucm.es; Tel.: +34-913-944-680

Received: 24 September 2018; Accepted: 10 October 2018; Published: 14 October 2018

Abstract: We reelaborate on the basic properties of $\mathcal{PT}$ symmetry from a geometrical perspective. The transfer matrix associated with these systems induces a Möbius transformation in the complex plane. The trace of this matrix classifies the actions into three types that represent rotations, translations, and parallel displacements. We find that a $\mathcal{PT}$ invariant system can be pictured as a complex conjugation followed by an inversion in a circle. We elucidate the physical meaning of these geometrical operations and link them with measurable properties of the system.

Keywords: $\mathcal{PT}$ symmetry; SL(2, $\mathbb{C}$); hyperbolic geometry

1. Introduction

In quantum theory, the Hamiltonian—and any other real-world observable—is represented by a Hermitian operator. This assumption ensures that the measurement of the energy always yields a real number. In addition, the time-evolution operator generated by a Hermitian Hamiltonian is unitary, which enforces the conservation of probabilities during the evolution of a quantum state.

Nonetheless, non-Hermitian potentials have been used to phenomenologically describe losses [1]. This is the case in open systems, with injecting sources and absorbing sinks, or in systems that decay, e.g., by spontaneous emission of photons from an excited level. The whole system still obeys conventional quantum mechanics; the non-Hermitian Hamiltonian only comes out as an effective subsystem within a projective subspace.

A crucial twist in this field occurred a few years ago, when Bender and coworkers [2–7] proposed the use of complex potentials that have neither parity ($\mathcal{P}$) nor time-reversal symmetry ($\mathcal{T}$), but retain combined $\mathcal{PT}$ invariance. They can display real energy eigenvalues, thus suggesting a credible generalization of quantum theory. Actually, by redefining the inner product, the time-evolution operator generated by such potentials could be unitary [8–10]. Moreover, they can also exhibit a spontaneous $\mathcal{PT}$ symmetry-breaking, at which the reality of the eigenvalues is lost [11–14].

This concept has prompted a continuing debate in several forefronts, including self-trapped modes [15], quantum field theories [16,17], Anderson localization [18–20], complex crystals [21–24], Lie algebras [25–27] and open quantum systems [28], to mention but a few.

The possibility of realizing $\mathcal{PT}$-symmetric potentials led to a flurry of activity in optics, for the paraxial wave equation is fully analogous to Scrödinger equation. The complex refractive index plays here the role of the potential, so they can be accomplished through a sensible inclusion of gain and loss regions. This has been experimentally observed [29]. Besides, $\mathcal{PT}$ synthetic materials can exhibit enthralling features; such as power oscillations [30], nonreciprocity of light propagation [31], Bloch oscillations [32], coherent perfect absorbers [33,34], nonlinear switching structures [35], or unidirectional invisibility [36–38].

All these issues are classical and, in a broad sense, they are effective models. However, in the quantum regime, Bender proposed two interesting applications related to quantum computation:

ultrafast quantum state transformation [39] and quantum state discrimination with single-shot measurement [40]. This also inspired ideas on shortcuts to adiabaticity [41,42], despite some subtleties [43].

Interesting as they are, these developments have one potential criticism: the physical interpretation of $\mathcal{PT}$ symmetry remains vague [44,45]. Our purpose here is to put forth a simple but fundamental geometrical characterization of the action of these systems.

To this end we resort to the time-honored transfer-matrix method [46]. Via the Möbius transformation [47–49], this matrix induces a rich geometry in the complex plane $\mathbb{C}$; its trace classifies the actions into three types that represent rotations, translations, or parallel displacements. For the case of $\mathcal{PT}$ symmetry, we argue that the transfer matrix may be understood as a point in the de Sitter space [50–52] and it may be pictured as a complex conjugation followed by an inversion in a circle. We also explore the physical meaning of these fundamental building blocks.

Our approach does not provide any benefit in terms of efficiency in solving practical problems. Rather, it provides a unifying framework to analyze the behavior of complex potentials, which, in our opinion, is of relevance for the field.

2. Basic Concepts on the Transfer Matrix

Let us first set the stage for our analysis. We consider the scattering of a particle of mass m by a local complex potential $V(x)$ defined on $\mathbb{R}$ [53–55]. The dynamics is determined by the time-independent Schrödinger equation

$$H\Psi(x) = \left[-\frac{d^2}{dx^2} + U(x)\right]\Psi(x) = \varepsilon\,\Psi(x)\,, \tag{1}$$

where $\varepsilon = 2mE/\hbar^2$ and $U(x) = 2mV(x)/\hbar^2$, with E the energy of the particle. We assume that $U(x) \to 0$ fast enough as $x \to \pm\infty$, so there exist independent solutions of (1) behaving asymptotically as

$$\Psi(x) = \begin{cases} A_+e^{+ikx} + A_-e^{-ikx} & x \to -\infty\,, \\ \\ B_+e^{+ikx} + B_-e^{-ikx} & x \to +\infty\,. \end{cases} \tag{2}$$

Here, $k = \sqrt{\varepsilon}$ is the wavenumber and the subscripts $+$ and $-$ discriminate right-moving modes $\exp(+ikx)$ from left-moving modes $\exp(-ikx)$, respectively.

The exact determination of $A_\pm$ and $B_\pm$ amounts to solving (1) with the suitable boundary conditions. This leads to two linear relations among the coefficients $A_\pm$ and $B_\pm$, which can be solved for any amplitude pair in terms of the other two. The transfer matrix [46] corresponds to specifying the relation between the wave amplitudes on both sides of the scatterer, viz,

$$\begin{pmatrix} A_+ \\ A_- \end{pmatrix} = \mathsf{M}\begin{pmatrix} B_+ \\ B_- \end{pmatrix}. \tag{3}$$

Obviously, M depends in a complicated way on the potential $U(x)$. Fortunately, we still can gain insights into the asymptotic behavior without explicitly calculating it. First, we apply (3) successively to a right-moving $[(A_+ = 1, B_- = 0)]$ and to a left-moving wave $[(A_+ = 0, B_- = 1)]$, both of unit amplitude:

$$\begin{pmatrix} 1 \\ \mathfrak{r}^\ell \end{pmatrix} = \mathsf{M}\begin{pmatrix} \mathfrak{t}^\ell \\ 0 \end{pmatrix}, \qquad \begin{pmatrix} 0 \\ \mathfrak{t}^r \end{pmatrix} = \mathsf{M}\begin{pmatrix} \mathfrak{r}^r \\ 1 \end{pmatrix}. \tag{4}$$

Here, $\mathfrak{t}^{\ell,r}$ and $\mathfrak{r}^{\ell,r}$ are the transmission and reflection coefficients for a wave incoming at the potential from the left and from the right, respectively [56].

Equation (4) can also be understood as the superposition of the two independent solutions

$$\Psi_k^\ell(x) \;=\; \begin{cases} e^{+ikx} + \mathfrak{r}^\ell(k)\, e^{-ikx} & x \to -\infty\,, \\ \\ \qquad\quad \mathfrak{t}^\ell(k)\, e^{+ikx} & x \to +\infty\,, \end{cases}$$
$$\Psi_k^r(x) \;=\; \begin{cases} \qquad\quad \mathfrak{t}^r(k)\, e^{-ikx} & x \to -\infty\,, \\ \\ e^{-ikx} + \mathfrak{r}^r(k)\, e^{+ikx} & x \to +\infty\,. \end{cases} \tag{5}$$

The wave function $\Psi_k^\ell(x)$ describes a wave incident from $-\infty$ [$\exp(+ikx)$] and the interaction with the potential produces a reflected wave [$\mathfrak{r}^\ell(k)\exp(-ikx)$] that escapes to $-\infty$ and a transmitted wave [$\mathfrak{t}^\ell(k)\exp(+ikx)$] that moves off to $+\infty$. The solution $\Psi_k^r(x)$ can be interpreted in a similar fashion.

The Wronskian of the solutions (5) is independent of x. Therefore, we can compute $W(\Psi_k^\ell, \Psi_k^r) = \Psi_k^\ell \Psi_k^{r\,\prime} - \Psi_k^{\ell\,\prime}\Psi_k^r$ first for $x \to -\infty$ and then for $x \to \infty$. The final results reads

$$\frac{i}{2k} W(\Psi_k^\ell, \Psi_k^r) = \mathfrak{t}^r(k) = \mathfrak{t}^\ell(k) \equiv \mathfrak{t}(k)\,, \tag{6}$$

which ensures that the transmission coefficient is always independent of the direction of the incident wave.

We can now get back to (4) and write the solution for M as (in what follows, to lighten notation, we omit the k dependence of the coefficients)

$$\mathsf{M} = \frac{1}{\mathfrak{t}} \begin{pmatrix} 1 & \mathfrak{r}^r \\ -\mathfrak{r}^\ell & \mathfrak{t}^2 - \mathfrak{r}^\ell \mathfrak{r}^r \end{pmatrix}. \tag{7}$$

It is direct to confirm that $\det \mathsf{M} = +1$, so $\mathsf{M} \in \mathrm{SL}(2, \mathbb{C})$, the group of 2×2 complex matrices with unit determinant [57].

3. Geometry of Transfer Matrices

Let us consider a generic matrix $\mathsf{M} \in \mathrm{SL}(2, \mathbb{C})$, we shall denote by

$$\mathsf{M} = \begin{pmatrix} a & b \\ c & d \end{pmatrix}, \tag{8}$$

with $a, b, c, d \in \mathbb{C}$ and $\det \mathsf{M} = ad - bc = 1$. The matrix M induces a mapping in $\mathbb{C}$ via a Möbius (or linear fractional) transformation [47–49]

$$z' = \frac{a\,z + b}{c\,z + d}\,. \tag{9}$$

From a physical perspective, (9) arises because the relevant variables are quotients of amplitudes (such as, e.g., A_+/A_-) rather than the amplitudes themselves. For each value of z, Equation (9) gives one and only one value of z'. There is no exception to this statement if we introduce the point at infinity: if $c \neq 0$, $z = -d/c$ is transformed into $z' = \infty$ and $z = \infty$ into $z' = a/c$. If $c = 0$, $z = \infty$ is transformed into $z' = \infty$.

Equation (9) can be inverted, obtaining

$$z = \frac{-d\,z' + b}{c\,z' - a}\,, \tag{10}$$

which is another Möbius transformation.

The fixed points are those that remain invariant under M; i.e., $z' = z$. They are given by

$$z_{\pm} = \frac{(a-d) \pm \sqrt{[\mathrm{Tr}(\mathsf{M})]^2 - 4}}{2c}\,, \tag{11}$$

and determined solely by the trace. We will be mostly interested in the case when $\mathrm{Tr}(\mathsf{M})$ is a real number, as it will happen for $\mathcal{PT}$ invariance. The Möbius transformations are then called hyperbolic, elliptic, or parabolic, according $[\mathrm{Tr}(\mathsf{M})]^2$ is greater than, lesser than, or equal to 4, respectively.

Equation (9) can be rewritten in a very suggestive form using the fixed points; namely,

$$\frac{z' - z_+}{z' - z_-} = K\,\frac{z - z_+}{z - z_-}\,, \tag{12}$$

where we have taken $c \neq 0$ (the case $c = 0$ can be treated similarly). The factor K is called the multiplier and its value is determined by

$$K + \frac{1}{K} = [\mathrm{Tr}(\mathsf{M})]^2 - 2\,. \tag{13}$$

If the quotients appearing in both sides of (12) are designated by Z' and Z, respectively, (9) can be compactly recast as $Z' = KZ$, so K determines all its properties. Writing this factor as $K = Ae^{i\theta}$ (with $A > 0$), it turns out that the aforementioned hyperbolic, elliptic, and parabolic actions appear as

$$Z' = A\,Z\,, \qquad Z' = e^{i\theta}\,Z\,, \qquad Z' = Z + c\,, \tag{14}$$

whose interpretation is clear. The hyperbolic action (with fixed points 0 and ∞) performs a stretching by a factor $A \neq 1$. Every straight line through the origin is transformed into itself and any circle with center at the origin is transformed into some other circle with center at the origin. The elliptic action is a rotation about the origin of angle θ. The straight lines and circles of the hyperbolic action have their roles interchanged. Finally, for the parabolic transformation (with only one fixed point), $K = 1$ and consists in parallel displacements. Every straight line parallel to the translation vector c is invariant. The only fixed point now is at infinity.

We next introduce the concept of the isometric circle [58], which has been used in several applications [59,60] and will play a fundamental role in our later developments. It is defined as the locus of points in the neighborhood of which lengths are unaltered in magnitude by the Möbius transformation. Since

$$\frac{\mathrm{d}z'}{\mathrm{d}z} = \frac{1}{(cz+d)^2}\,, \tag{15}$$

the isometric circle is ($c \neq 0$)

$$|cz + d| = 1\,. \tag{16}$$

Similarly, the inverse transformation (10) has the isometric circle

$$|cz' - a| = 1\,. \tag{17}$$

The isometric circle of the direct transformation, C_d, has its center at $O_d = -d/c$ and radius $R_c = 1/|c|$; the isometric circle of the inverse transformation C_i, has its center at $O_i = a/c$ and the same radius. Actually, the Möbius transformation carries the isometric circle C_d into C_i. As a point moves counterclockwise around C_d, the corresponding point moves clockwise around C_i.

The central result for our purposes is that any Möbius transformation with real trace is equivalent to an inversion in C_d followed by a reflection in L [58], which is the perpendicular bisector of the line

segment joining the centers of C_d and C_i. This can be easily intuited from the sketch in Figure 1. To prove it in a quantitative way, we explicitly decompose (9) in two successive steps [59]

$$z_d^* = -\frac{\left(\frac{d}{c}\right)^* z + \frac{|d|^2-1}{|c|^2}}{z+\frac{d}{c}}, \qquad z' = \frac{-\left(\frac{a+d}{c}\right) z_d^* + \frac{|a|^2-|d|^2}{|c|^2}}{\left(\frac{a+d}{c}\right)^*}. \tag{18}$$

The first one, $z \mapsto z_d$, corresponds to the inversion in the circle C_d, whereas the second one, $z_d \mapsto z'$ is the reflection in the line L. The same result holds if, instead of inverting in C_d and then reflecting in L, we reflect in L and then invert in C_i, as it is also indicated in Figure 1.

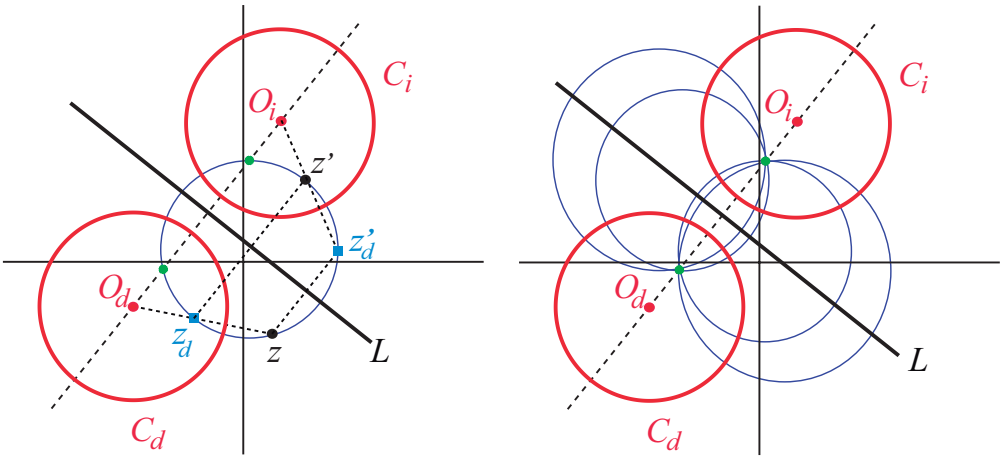

Figure 1. (**Left**) The isometric method for a Möbius transformation of the hyperbolic type. We have plotted the isometric circles for the direct (C_d) and the inverse (C_i) transformations, with centers in O_d and O_i, respectively. The fixed points are marked in green and L is the reflection line. z and z' are the points related by M, whereas z_d is the point obtained by an inversion of z respect to C_d and z'_d the reflected of z by L. The inversion of z'_d respect to C_i gives z'. (**Right**) Two typical families of fixed lines for the same transformation.

We recall that if C is a circle with center w and radius r, an inversion in the circle C maps the point ζ into the point ζ' along the same radius in such a way that the product of distances from the center w satisfies

$$|\zeta' - w|\,|\zeta - w| = r^2 \tag{19}$$

so that

$$\zeta'^* = w^* + \frac{r^2}{\zeta - w}. \tag{20}$$

For the hyperbolic transformations one fixed point is within C_d, the other is outside; for the elliptic transformation both fixed points, and for the parabolic transformation the single fixed point, are on C_d, as can be seen in Figure 2. Identical statements are true for C_i for similar reasons. In the elliptic transformation C_d and C_i intersect and L is the common chord. The points of intersection are fixed points. In the parabolic transformation, L is the common tangent to C_d and C_i at their point of tangency, which is precisely the fixed point.

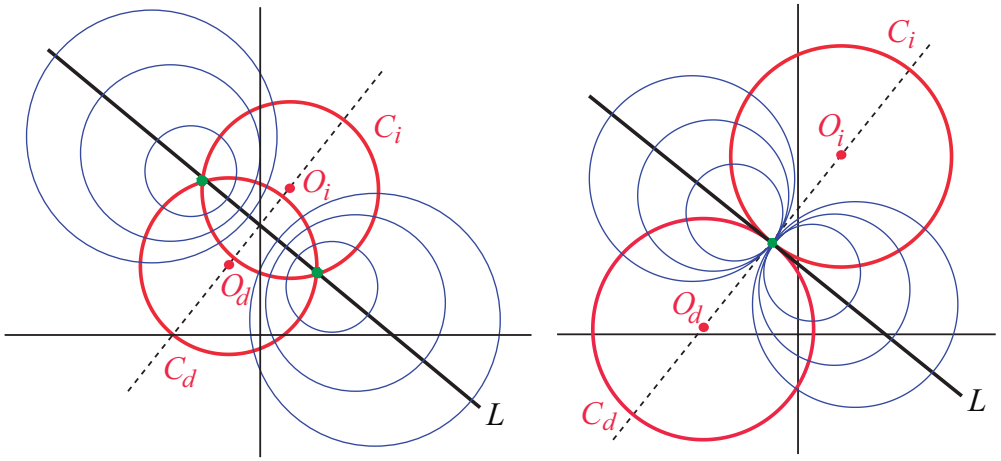

Figure 2. Families of fixed lines for elliptic (**left**) and parabolic (**right**) Möbius transformations. We show the isometric circles C_d and C_i and their centers O_d and O_i. The fixed points are marked in green.

Each one of the transformations we are considering has a one-parameter family of fixed circles, including, as we have discussed, the line joining the centers of C_d and C_i. These circles are relevant because once we know the initial point z is in one of them, the transformed point z' is also in that same circle. The family is easily constructed [58]: it consists of circles with centers on L orthogonal to C_d. For, being orthogonal to C_d, such a circle is transformed into itself by an inversion in C_d; and a reflection in L, a diameter, transforms it again into itself. Each fixed circle is also orthogonal to C_i from symmetry. These families are shown in Figures 1 and 2 for the three kind of transformations.

To interpret the physical significance of the inversion, let us interchange incoming and outgoing fields, which is just reversing the time arrow. Since for a given forward-traveling field A_+, the conjugate A_+^* represents a backward phase-conjugate wave of the original field, the time-reversal operation can be viewed in this context as the transformation

$$z \mapsto \frac{1}{z^*}\,, \tag{21}$$

that is, an inversion in the unit circle.

4. Geometry of $\mathcal{PT}$-Invariant Transfer Matrices

We impose now the additional conditions of $\mathcal{PT}$-symmetry on the transfer matrix. We remind that the parity transformation is a space reflection, so that $x \mapsto -x$ and $p \mapsto -p$. The action is

$$\Psi(x) \overset{\mathcal{P}}{\longmapsto} \Psi(-x)\,. \tag{22}$$

The time reversal inverts the sense of time, so that $x \mapsto x$, $p \mapsto -p$ and $i \mapsto -i$. The operator $\mathcal{T}$ implementing this transformation is antiunitary:

$$\Psi(x) \overset{\mathcal{T}}{\longmapsto} \Psi^*(x)\,. \tag{23}$$

Therefore, under a combined $\mathcal{PT}$ transformation, we have

$$\Psi(x) \overset{\mathcal{PT}}{\longmapsto} \Psi^*(-x)\,. \tag{24}$$

The transfer matrix of the $\mathcal{PT}$-transformed system, we denote by $\mathsf{M}^{(\mathcal{PT})}$, has to fulfil

$$\begin{pmatrix} B_+^* \\ B_-^* \end{pmatrix} = \mathsf{M}^{(\mathcal{PT})} \begin{pmatrix} A_+^* \\ A_-^* \end{pmatrix}\,. \tag{25}$$

By comparing with (3), we get that $\mathsf{M}^{(\mathcal{PT})} = (\mathsf{M}^{-1})^*$, which implies

$$M_{11} \overset{\mathcal{PT}}{\longmapsto} M_{22}^*\,, \qquad M_{12} \overset{\mathcal{PT}}{\longmapsto} -M_{12}^*\,, \qquad M_{21} \overset{\mathcal{PT}}{\longmapsto} -M_{21}^*\,, \qquad M_{22} \overset{\mathcal{PT}}{\longmapsto} M_{11}^*\,. \tag{26}$$

We shall denote henceforth the $\mathcal{PT}$-invariant transfer matrix by $\mathcal{M}$. It must hold then

$$\mathcal{M}^{-1} = \mathcal{M}^*\,, \tag{27}$$

which imposes the constraints

$$\mathrm{Re}\left(\frac{\mathfrak{r}^\ell}{\mathfrak{t}}\right) = \mathrm{Re}\left(\frac{\mathfrak{r}^r}{\mathfrak{t}}\right) = 0\,. \tag{28}$$

In consequence, the general form of a $\mathcal{PT}$-invariant transfer matrix is

$$\mathcal{M} = \begin{pmatrix} x_1 + ix_2 & i(x_3 + x_0) \\ i(x_3 - x_0) & x_1 - ix_2 \end{pmatrix}\,, \tag{29}$$

with

$$x_1 = \mathrm{Re}\left(\frac{1}{\mathfrak{t}}\right), \qquad x_2 = -\mathrm{Im}\left(\frac{1}{\mathfrak{t}}\right), \qquad x_3 = \frac{\mathfrak{r}^\ell - \mathfrak{r}^r}{2i\mathfrak{t}}, \qquad x_0 = \frac{\mathfrak{r}^r + \mathfrak{r}^\ell}{2i\mathfrak{t}}\,. \tag{30}$$

The condition $\det \mathcal{M} = 1$ gives

$$x_1^2 + x_2^2 + x_3^2 - x_0^2 = 1\,, \tag{31}$$

so that we can look at $\mathcal{M}$ as defining a point in a single-sheeted unit hyperboloid, which is known as the de Sitter space dS_3 [50–52].

The fixed points of $\mathcal{M}$ are

$$z_\pm = \frac{x_2 \mp i\sqrt{x_1^2 - 1}}{x_3 - x_0}\,. \tag{32}$$

For hyperbolic actions they are conjugate, whereas for the elliptic case, both points are real.

Let us focus for the time being on this elliptic case, as the other two can be worked out much in the same way. The reflection line L is now the real axis and the associated reflection is then a complex conjugation. To be specific, we shall resort to the simple model of a single one-dimensional $\mathcal{PT}$-symmetric slab of total length h with balanced refractive index $n = 3 \pm 0.005i$ in each half [34]. By adjusting h we can get a typical case of transfer matrix such as, e.g.,

$$\mathcal{M} = \begin{pmatrix} 0.7779 - 0.1263i & -0.2507i \\ -1.5116i & 0.7779 + 0.1263i \end{pmatrix}\,. \tag{33}$$

The fixed points are $z_+ = -0.3322$ and $z_- = 0.4993$, whereas the isometric circles are centered at $O_d = 0.0836 - 0.5146i$ and $O_i = 0.0836 + 0.5146i$, with radii $R_d = R_i = 0.6616$.

As one can appreciate in Figure 3, the action of $\mathcal{M}$, mapping the point z onto z', can be equivalently decomposed either in the sequence $z \mapsto z'^* \mapsto z'$ (inversion in C_d and complex conjugation) or $z \mapsto z^* \mapsto z'$ (complex conjugation and inversion in C_i). Please note that C_d and C_i are complex conjugate each other.

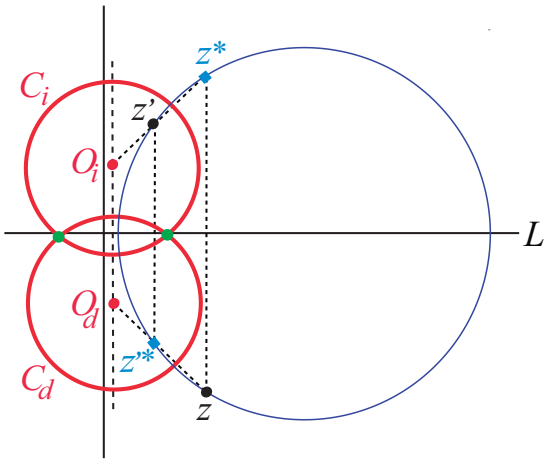

Figure 3. The isometric method as in Figure 2, but now applied to an elliptic $\mathcal{PT}$-invariant transfer matrix $\mathcal{M}$ given in (33) . We show again the isometric circle for the direct (C_d) and the inverse (C_i) transformations, with centers in O_d and O_i, respectively. The symmetry line L coincides with the real axis, so the corresponding reflection reduces to a complex conjugation.

Let us conclude by treating a particularly interesting example. We take $x_0 = -x_3$, so we have a lower triangular matrix

$$\mathcal{M} = \begin{pmatrix} \exp(i\varphi) & 0 \\ i2x_3 & \exp(-i\varphi) \end{pmatrix} . \tag{34}$$

Both isometric circles C_d and C_i pass through the origin, with centers at $O_d = e^{i\varphi}/(i2x_3)$ and $O_i = -e^{-i\varphi}/(i2x_3)$ and radius $1/(2x_3)$. Again, the mapping $z \mapsto z'$ induced by $\mathcal{M}$ can be decomposed as before. When $\varphi = 0$, according to Equation (30), this potential satisfies $\mathfrak{r}^\ell = 0$ and $\mathfrak{t} = 1$, so it is left invisible.

5. Concluding Remarks

Geometry constitutes the natural arena to formulate numerous physical ideas. In this paper, we have worked out a geometric scenario of $\mathcal{PT}$-invariant systems. More specifically, we have reduced the action of any of these systems to a complex conjugation and an inversion. We have given an interpretation of these actions and expressed them in terms of the physical parameters of the system. The behavior analyzed here is relevant not only in optics, but in all those fields in which the transfer matrix is the method of choice.

Author Contributions: Both authors contributed equally to all aspects of preparing this manuscript.

Funding: Financial support from the Spanish MINECO (Grant No. FIS2015-67963-P) is gratefully acknowledged.

Acknowledgments: We acknowledge illuminating discussions with José María Montesinos.

Conflicts of Interest: The authors declare no conflicts of interest.

References

1. Muga, J.G.; Palao, J.P.; Navarro, B.; Egusquiza, I.L. Complex absorbing potentials. *Phys. Rep.* **2004**, *395*, 357–426. [CrossRef]
2. Bender, C.M.; Boettcher, S. Real spectra in non-Hermitian Hamiltonians having $\mathcal{PT}$ symmetry. *Phys. Rev. Lett.* **1998**, *80*, 5243–5246. [CrossRef]
3. Bender, C.M.; Boettcher, S.; Meisinger, P.N. $\mathcal{PT}$-symmetric quantum mechanics. *J. Math. Phys.* **1999**, *40*, 2201–2229. [CrossRef]
4. Bender, C.M.; Brody, D.C.; Jones, H.F. Complex extension of quantum mechanics. *Phys. Rev. Lett.* **2002**, *89*, 270401. [CrossRef] [PubMed]

5. Bender, C.M.; Brody, D.C.; Jones, H.F. Must a Hamiltonian be Hermitian? *Am. J. Phys.* **2003**, *71*, 1095–1102. [CrossRef]
6. Bender, C.M. Making sense of non-Hermitian Hamiltonians. *Rep. Prog. Phys.* **2007**, *70*, 947–1018. [CrossRef]
7. Bender, C.M.; Mannheim, P.D. $\mathcal{PT}$ symmetry and necessary and sufficient conditions for the reality of energy eigenvalues. *Phys. Lett. A* **2010**, *374*, 1616–1620. [CrossRef]
8. Mostafazadeh, A. Exact $\mathcal{PT}$-symmetry is equivalent to Hermiticity. *J. Phys. A* **2003**, *36*, 7081. [CrossRef]
9. Mostafazadeh, A. Pseudo-Hermiticity and generalized $\mathcal{PT}$- and $\mathcal{CPT}$-symmetries. *J. Math. Phys.* **2003**, *44*, 974–989. [CrossRef]
10. Wang, Q.H.; Chia, S.Z.; Zhang, J.H. PT-symmetry as a generalization of Hermiticity. *J. Phys. A* **2010**, *43*, 295301. [CrossRef]
11. Delabaere, E.; Pham, F. Eigenvalues of complex Hamiltonians with $\mathcal{PT}$-symmetry. *Phys. Lett. A* **1998**, *250*, 25–28. [CrossRef]
12. Klaiman, S.; Günther, U.; Moiseyev, N. Visualization of branch points in $\mathcal{PT}$-symmetric waveguides. *Phys. Rev. Lett.* **2008**, *101*, 080402. [CrossRef] [PubMed]
13. Guo, A.; Salamo, G.J.; Duchesne, D.; Morandotti, R.; Volatier-Ravat, M.; Aimez, V.; Siviloglou, G.A.; Christodoulides, D.N. Observation of $\mathcal{PT}$-symmetry breaking in complex optical potentials. *Phys. Rev. Lett.* **2009**, *103*, 093902. [CrossRef] [PubMed]
14. Levai, G. Spontaneous breakdown of $\mathcal{PT}$ symmetry in the complex Coulomb potential. *Pramana* **2009**, *73*, 329–335.
15. Musslimani, Z.H.; Makris, K.G.; El-Ganainy, R.; Christodoulides, D.N. Optical solitons in $\mathcal{PT}$ periodic potentials *Phys. Rev. Lett.* **100**, 030402.
16. Bender, C.M.; Brody, D.C.; Jones, H.F. Extension of $\mathcal{PT}$-symmetric quantum mechanics to quantum field theory with cubic interaction. *Phys. Rev. D* **2004**, *70*, 025001. [CrossRef]
17. Jones, H.F. Equivalent Hamiltonians for $\mathcal{PT}$-symmetric versions of dual 2D field theories. *J. Phys. A* **2006**, *39*, 10123–10132. [CrossRef]
18. Goldsheid, I.Y.; Khoruzhenko, B.A. Distribution of eigenvalues in non-Hermitian Anderson models. *Phys. Rev. Lett.* **1998**, *80*, 2897–2900. [CrossRef]
19. Heinrichs, J. Eigenvalues in the non-Hermitian Anderson model. *Phys. Rev. B* **2001**, *63*, 165108. [CrossRef]
20. Molinari, L.G. Non-Hermitian spectra and Anderson localization. *J. Phys. A* **2009**, *42*, 265204. [CrossRef]
21. Bender, C.M.; Dunne, G.V.; Meisinger, P.N. Complex periodic potentials with real band spectra. *Phys. Lett. A* **1999**, *252*, 272–276. [CrossRef]
22. Jones, H.F. The energy spectrum of complex periodic potentials of Kronig–Penney type. *Phys. Lett. A* **1999**, *262*, 242–264. [CrossRef]
23. Znojil, M. $\mathcal{PT}$-symmetric square well. *Phys. Lett. A* **2001**, *285*, 7–10. [CrossRef]
24. Ahmed, Z. Energy band structure due to a complex, periodic, $\mathcal{PT}$-invariant potential. *Phys. Lett. A* **2001**, *286*, 231–235. [CrossRef]
25. Bagchia, B.; Quesne, C. sl(2, C) as a complex Lie algebra and the associated non-Hermitian Hamiltonians with real eigenvalues. *Phys. Lett. A* **2000**, *273*, 285–292. [CrossRef]
26. Bender, C.M.; Klevansky, S.P. $\mathcal{PT}$-symmetric representations of fermionic algebras. *Phys. Rev. A* **2011**, *84*, 024102. [CrossRef]
27. Cherbal, O.; Trifonov, D.A. Extended $\mathcal{PT}$- and $\mathcal{CPT}$-symmetric representations of fermionic algebras. *Phys. Rev. A* **2012**, *85*, 05212. [CrossRef]
28. Rotter, I. A non-Hermitian Hamilton operator and the physics of open quantum systems. *J. Phys. A* **2009**, *42*, 153001. [CrossRef]
29. Ruter, C.E.; Makris, K.G.; El-Ganainy, R.; Christodoulides, D.N.; Segev, M.; Kip, D. Observation of parity-time symmetry in optics. *Nat. Phys.* **2010**, *6*, 192–195. [CrossRef]
30. Makris, K.G.; El-Ganainy, R.; Christodoulides, D.N.; Musslimani, Z.H. Beam dynamics in $\mathcal{PT}$ symmetric optical lattices. *Phys. Rev. Lett.* **2008**, *100*, 103904. [CrossRef] [PubMed]
31. Zheng, M.C.; Christodoulides, D.N.; Fleischmann, R.; Kottos, T. $\mathcal{PT}$ optical lattices and universality in beam dynamics. *Phys. Rev. A* **2010**, *82*, 010103. [CrossRef]
32. Longhi, S. Bloch oscillations in complex crystals with $\mathcal{PT}$ symmetry. *Phys. Rev. Lett.* **2009**, *103*, 123601. [CrossRef] [PubMed]
33. Longhi, S. $\mathcal{PT}$-symmetric laser absorber. *Phys. Rev. A* **2010**, *82*, 031801. [CrossRef]

34. Chong, Y.D.; Ge, L.; Stone, A.D. $\mathcal{PT}$-symmetry breaking and laser-absorber modes in optical scattering systems. *Phys. Rev. Lett.* **2011**, *106*, 093902. [CrossRef] [PubMed]
35. Sukhorukov, A.A.; Xu, Z.; Kivshar, Y.S. Nonlinear suppression of time reversals in $\mathcal{PT}$-symmetric optical couplers. *Phys. Rev. A* **2010**, *82*, 043818. [CrossRef]
36. Ahmed, Z.; Bender, C.M.; Berry, M.V. Reflectionless potentials and $\mathcal{PT}$ symmetry. *J. Phys. A* **2005**, *38*, L627–L630. [CrossRef]
37. Lin, Z.; Ramezani, H.; Eichelkraut, T.; Kottos, T.; Cao, H.; Christodoulides, D.N. Unidirectional invisibility dnduced by $\mathcal{PT}$-symmetric periodic structures. *Phys. Rev. Lett.* **2011**, *106*, 213901. [CrossRef] [PubMed]
38. Longhi, S. Invisibility in $\mathcal{PT}$-symmetric complex crystals. *J. Phys. A* **2011**, *44*, 485302. [CrossRef]
39. Bender, C.M.; Brody, D.C.; Jones, H.F.; Meister, B.K. Faster than Hermitian quantum mechanics. *Phys. Rev. Lett.* **2007**, *98*, 040403. [CrossRef] [PubMed]
40. Bender, C.M.; Brody, D.C.; Caldeira, J.; Günther, U.; Meister, B.K.; Samsonov, B.F. $\mathcal{PT}$-symmetric quantum state discrimination. *Philos. Transact. A Math. Phys. Eng. Sci.* **2013**, *371*, 20120160. [CrossRef] [PubMed]
41. Ibáñez, S.; Martínez-Garaot, S.; Chen, X.; Torrontegui, E.; Muga, J.G. Shortcuts to adiabaticity for non-Hermitian systems. *Phys. Rev. A* **2011**, *84*, 023415. [CrossRef]
42. Torosov, B.T.; Della Valle, G.; Longhi, S. Non-Hermitian shortcut to adiabaticity. *Phys. Rev. A* **2013**, *87*, 052502. [CrossRef]
43. Lee, Y.C.; Hsieh, M.H.; Flammia, S.T.; Lee, R.K. Local $\mathcal{PT}$ symmetry violates the no-signaling principle. *Phys. Rev. Lett.* **2014**, *112*, 130404. [CrossRef] [PubMed]
44. Weigert, S. The physical interpretation of $\mathcal{PT}$-invariant systems. *Czech J. Phys.* **2004**, *54*, 1139–1142. [CrossRef]
45. Jin, L.; Song, Z. A physical interpretation for the non-Hermitian Hamiltonian. *J. Phys. A* **2011**, *44*, 375304. [CrossRef]
46. Sánchez-Soto, L.L.; Monzón, J.J.; Barriuso, A.G.; Cariñena, J. The transfer matrix: A geometrical perspective. *Phys. Rep.* **2012**, *513*, 191–227. [CrossRef]
47. Needham, T. *Visual Complex Analysis*; Oxford University Press: Oxford, UK, 1997.
48. Anderson, J.W. *Hyperbolic Geometry*; Springer: New York, NY, USA, 1999.
49. Ratcliffe, J.G. *Foundations of Hyperbolic Manifolds*; Springer: Berlin, Germany, 2006.
50. O'Neill, B. *Semi-Riemannian Geometry with Applications to Relativity*; Academic Press: London, UK, 1983.
51. Moschella, U. The de Sitter and anti-de Sitter sightseeing tour. In Proceedings of the 20th Seminaire Poincaré, Paris, France, 21 November 2005; pp.1–12.
52. Monzón, J.J.; Barriuso, A.G.; Montesinos-Amilibia, J.M.; Sánchez-Soto, L.L. Geometrical aspects of $\mathcal{PT}$-invariant transfer matrices. *Phys. Rev. A* **2013**, *87*, 012111. [CrossRef]
53. Mostafazadeh, A. Spectral Singularities of Complex Scattering Potentials and Infinite Reflection and Transmission Coefficients at Real Energies. *Phys. Rev. Lett.* **2009**, *102*, 220402. [CrossRef] [PubMed]
54. Cannata, F.; Dedonder, J.P.; Ventura, A. Scattering in $\mathcal{PT}$-symmetric quantum mechanics. *Ann. Phys.* **2007**, *322*, 397–433. [CrossRef]
55. Ahmed, Z. New features of scattering from a one-dimensional non-Hermitian (complex) potential. *J. Phys. A* **2012**, *45*, 032004. [CrossRef]
56. Boonserm, P.; Visser, M. One dimensional scattering problems: A pedagogical presentation of the relationship between reflection and transmission amplitudes. *Thai J. Math.* **2010**, *8*, 83–97.
57. Mostafazadeh, A.; Mehri-Dehnavi, H. Spectral singularities, biorthonormal systems and a two-parameter family of complex point interactions. *J. Phys. A* **2009**, *42*, 125303. [CrossRef]
58. Ford, L.R. *Automorphic Functions*; AMS Chelsea Publishing: New York, NY, USA, 1972.
59. Bolinder, E.F. *Impedance and Power Transformations by the Isometric Circle Method and Non-Euclidean Hyperbolic Geometry*; Technical Report; MIT: Cambridge, MA, USA, 1957.
60. Rudolph, J.G.; Cheng, D.K. Isometric-circle interpretation of bilinear transformation and its application to VSWR minimization. *Radio Sci.* **1965**, *69D*, 1271–1283. [CrossRef]